

Robert Pasquarelli was born in Pittsburgh, PA. He obtained a B.S. in Chemistry from the Rochester Institute of Technology. During his undergraduate career, he held two SULI internships at the National Renewable Energy Laboratory (NREL) in the summers of 2006 and 2007. He is currently pursuing a Ph.D. in materials science at the Colorado School of Mines and is conducting his thesis research at NREL under David Ginley and Ryan O'Hayre. He enjoys hiking, biking, and graphic design.

Calvin Curtis is a senior scientist at the National Renewable Energy Laboratory (NREL). He earned his BS in chemistry at Harvey Mudd

College and his Ph.D. in inorganic chemistry from the University of California at Berkeley. After postdoctoral work at CalTech, he joined the technical staff at the Solar Energy Research Institute (now NREL) in 1980. His research interests include the synthesis of photovoltaic materials and semiconductor nanostructures from organometallic precursors, inkjet printing of electronic materials and metals using organometallic inks, hydrothermal synthesis of novel metal oxide nanostructures, and transition metal hydride thermodynamics. He is a co-inventor on 10 patents in the areas of synthesis and surface modification of nanoparticles, ink formulation and film deposition, and the author of over 50 refereed publications.

INKJET PRINTING OF NICKEL AND SILVER METAL SOLAR CELL CONTACTS

ROBERT PASQUARELLI, CALVIN CURTIS, AND MAIKEL VAN HEST

ABSTRACT

With about 125,000 terawatts of solar power striking the earth at any given moment, solar energy may be the only renewable energy resource with enough capacity to meet a major portion of our future energy needs. Thin-film technologies and solution deposition processes seek to reduce manufacturing costs in order to compete with conventional coal-based electricity. Inkjet printing, as a derivative of the direct-write process, offers the potential for low-cost, material-efficient deposition of the metals for photovoltaic contacts. Advances in contact metallizations are important because they can be employed on existing silicon technology and in future-generation devices. We report on the atmospheric, non-contact deposition of nickel (Ni) and silver (Ag) metal patterns on glass, Si, and ZnO substrates at 180–220°C from metal-organic precursor inks using a Dimatix inkjet printer. Near-bulk conductivity Ag contacts were successfully printed up to 4.5 μm thick and 130 μm wide on the silicon nitride antireflective coating of silicon solar cells. Thin, high-resolution Ni adhesion-layer lines were printed on glass and zinc oxide at 80 μm wide and 55 nm thick with a conductivity two orders of magnitude less than the bulk metal. Additionally, the ability to print multi-layered metallizations (Ag on Ni) on transparent conducting oxides was demonstrated and is promising for contacts in copper-indium-diselenide (CIS) solar cells. Future work will focus on further improving resolution, printing full contact devices, and investigating copper inks as a low-cost replacement for Ag contacts.

INTRODUCTION

With about 125,000 terawatts of solar power striking the earth at any given moment, solar energy may be the only renewable energy resource with enough capacity to meet a major portion of our future energy needs [1]. However, the key issue is cost. In order to compete with conventionally coal-based electricity, the U.S. Department of Energy's Solar America Initiative seeks to drive down the price of solar electricity to less than \$0.10 per kWh by 2015. Second-generation solar cells seek to reduce manufacturing costs through thin-film technology, process optimization, and minimizing material usage. In these devices, liquid precursor deposition methods (including spin coating, spray deposition, and inkjet printing) are attractive because the equipment required is simple and inexpensive, the methods are scalable to large substrate sizes, and they are carried out under atmospheric conditions. Inkjet printing, as a derivative of direct-write processing, offers further advantages including high material usage efficiency, non-contact processing for use with fragile thin-film substrates, and the elimination of photolithography [2].

Inkjet printing is quickly becoming an alternative to existing deposition methods and has wide-range potential in both inorganic and organic photovoltaic and electronic materials. With the appropriate inks, all the features of a solar cell, including the absorber, dopants, transparent conductor, and front and rear metal contacts, could be sprayed or directly printed. Advances in contact metallizations are important because they can be employed on existing silicon technology and in future-generation devices. As such, the initial thrust and focus of this paper is on the materials used for front metal contacts. At present, inkjets are capable of line resolutions less than 20 μm , which is two to four times better than the current method of screen printing [3]. High resolution (narrower contact lines) means more absorber material is exposed to sunlight and thus higher conversion efficiency can be obtained. Additionally, unlike screen printing, direct-write is a no-waste approach, which is both environmentally- and cost-friendly.

The ink consists of two major components: the appropriate precursor and the carrier (an organic solvent). The precursor is the compound that decomposes into the desired material or

metal. Additionally, the content of the ink can be easily tailored by addition of binders, adhesion promoters, surfactants, reducing agents, and dopants. Composition is important because it influences the way in which the ink is jetted and adheres to the substrate, the profile and resolution of the line, and the material/metal formation. The ink is printed onto a heated substrate in the desired pattern. At the appropriate temperature, the metallic film forms following decomposition of the precursor and evaporation of the solvent. Byproducts of decomposition leave as gases, resulting in contaminant-free films.

Inkjet printing allows for multilayer structures and thus is well-suited for contact layers, which are often multicomponent. Silver (Ag) is primarily used as the contact metal because of its high conductivity. Ideally, less expensive copper (Cu) would replace Ag as the contact. The printing approach for these contacts is dependent on the surface material. As such, surface modifying agents and adhesion inks have been developed to improve contact formation and surface adhesion. For example, silicon (Si) cells are coated with an anti-reflective (AR) layer of silicon nitride. The Ag contact can be printed onto a previously printed layer of fire-through ink, which when heated etches through the AR coating to expose the Si to the contact [4]. In next-generation copper-indium-diselenide (CIS) cells, the top layer is a transparent conducting oxide (TCO), which acts as both a conductor and a window to allow light to pass through to the absorbing layer. For these devices, a thin layer of nickel (Ni) is first applied to the TCO to create good adhesion between the TCO and contact. A typical CIS structure is depicted in Figure 1. Ag diffusion into the absorber layer can detrimentally affect efficiency, particularly for CIS. Therefore, in addition to acting as an adhesion layer, the Ni serves the essential role of a diffusion barrier [5].

We report on the inkjet printing of the Ag contact and Ni adhesion layer from proprietary inks developed at the National Renewable Energy Laboratory (NREL). Inkjet printing was chosen

over spray deposition because it is spatially selective and drop-on-demand, which is ideal for depositing contact grid patterns. The specific goals of this research were to optimize printing parameters and ink formulations to achieve highly conductive lines with good adhesion and high resolution. For the Ni adhesion layer, the target was to make each line as thin and narrow as possible while maintaining uniformity (no breaks, beading, or large profile variations). For the Ag contact layer, the target was a thicker (10 μm), narrow line with near bulk-material conductivity. The supporting Ni layer would ideally govern the Ag line width and profile.

MATERIALS AND METHODS

Inkjet System. Printing was performed using a Dimatix Materials Printer (Fujifilm Dimatix, Santa Clara, CA), as shown in Figure 2. The ink cartridge contains a piezoelectric material behind each ink nozzle. When a voltage is applied to the material, it changes shape, which results in a pressure pulse that forces a droplet of ink out of the nozzle. The cartridge consists of 16 nozzles with 10-picoliter drop volume. The Dimatix system consists of a print head positioned above a heatable platen on a moving stage. A programmable hotplate was constructed and mounted to the platen to provide a wider range of substrate temperatures (up to 400°C). The user has control over several parameters to optimize printing, including ink and substrate temperature, individual jet firing voltage (to tune drop velocity), firing frequency, and drop spacing.

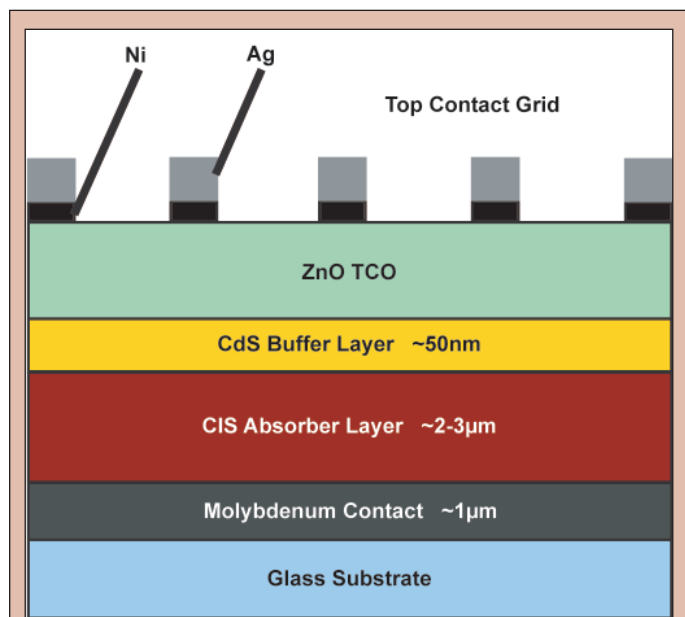


Figure 1. Schematic cross-sectional view of a substrate configuration device.

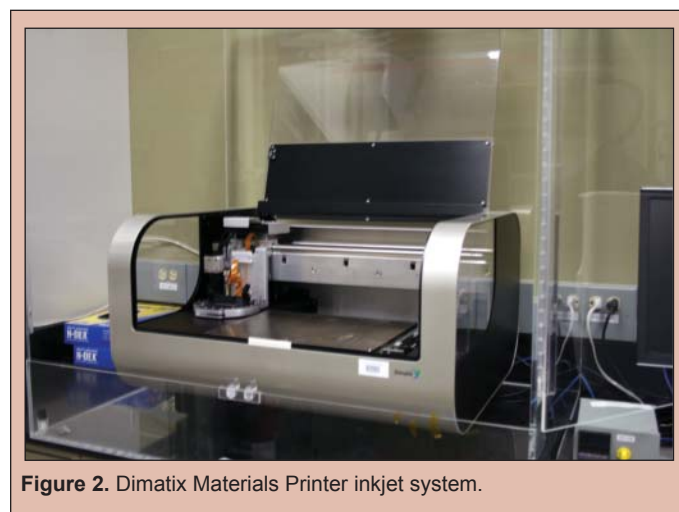


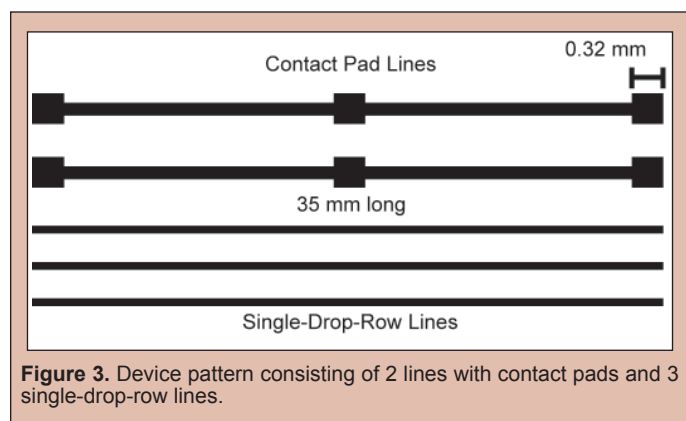
Figure 2. Dimatix Materials Printer inkjet system.

Inks. Metallization inks consisted of the precursor and additives dissolved in organic solvents (NREL proprietary compositions). Inks were filtered through a 0.2 μm syringe filter to remove particulates that would clog the nozzles and stored in their respective cartridges at room temperature. The Ni ink was stable for several months. The Ag ink was stored away from light to avoid decomposition, and the cartridge was covered with aluminum foil to avoid exposure to light during printing. The Ag ink began to discolor, indicating gradual decomposition, after a couple of weeks.

General Procedures. The Ni ink was printed over a substrate temperature range of 140 to 180°C, over a drop spacing range of 10 to 50 μm , and from 1 to 10 layers. Two printing approaches

were explored. The Ni Wet Print approach consists of printing a wet line at 140°C, and after printing, increasing to 180°C to induce decomposition and solvent evaporation. The Ni Hot Print approach involves printing the line at sufficient temperature (180°C) to simultaneously produce decomposition and evaporation as printing occurs. Glass microscope slides and thin films of ZnO on glass were used as substrates. The Ag ink was test printed between 155 and 220°C, over a drop spacing range of 20 to 70 μm, and from 1 to 200 layers. The ink was printed on four separate surfaces: (a) glass slides, (b) Ni printed lines, (c) 0.125 mm thick Ni foil, and (d) the silicon nitride AR coated side of Evergreen Solar silicon string ribbon.

Two printing patterns were used. Initial studies were performed on a pattern consisting of five lines with increasing incremental widths of 20 μm. The second pattern was used to test device features, consisting of single-drop-row lines for fine resolution tests and wider lines with square pads at the ends for performing conductivity measurements (Figure 3).



Substrate surface temperature was monitored with a type-J thermocouple thermometer prior to printing. Line thickness, width, and cross-sectional area were measured using a Dektak 8 profilometer. A Nikon Eclipse LV 100 camera equipped microscope was used to image lines and assess line quality. X-ray diffraction (XRD) studies were performed on a Bruker AXS D8 Discovery System. Resistivity, calculated using the equation below, was determined by using a four-point probe microscope station to measure voltage (V) and current (I).

$$\text{Resistivity } (\Omega \cdot \text{cm}) = \frac{V}{I} \cdot \frac{\text{cross-sectional area of line}}{\text{length of line between probes}}$$

RESULTS

Four layers of Ni ink were printed on glass using the five-line pattern to observe changes in line profile as a function of drop spacing. Drop spacing was varied in 5-μm increments from 10 to 50 μm. The average line width and thickness of Hot and Wet printed Ni ink at the determined optimal drop spacing of 30 μm was plotted in Figure 4. Using this drop spacing and the Hot Print approach, Ni was printed from 1 to 10 layers using the device pattern. The average width and thickness of these single-drop-row lines on glass was plotted in Figure 5A as a function of the number of layers

printed. For the line profile data, width refers to the resolution (narrowness) of the line, and thickness refers to line height. Line width and thickness measurements from the five-line pattern are averages of profilometry readings at two points per line. Device pattern data with single-drop-row lines represent the average of six measurements, two per line over three lines to test variation within a line and reproducibility of lines. Microscope images of Ni contact pad lines Hot printed on glass and ZnO are provided in Figure 6.

Ag was printed from 1 to 200 layers using the device pattern on AR coated Si ribbon at 215°C with an optimized 35-μm drop spacing and an initial ink temperature of 45°C. The average width and thickness of the single-drop-row lines was plotted in Figure

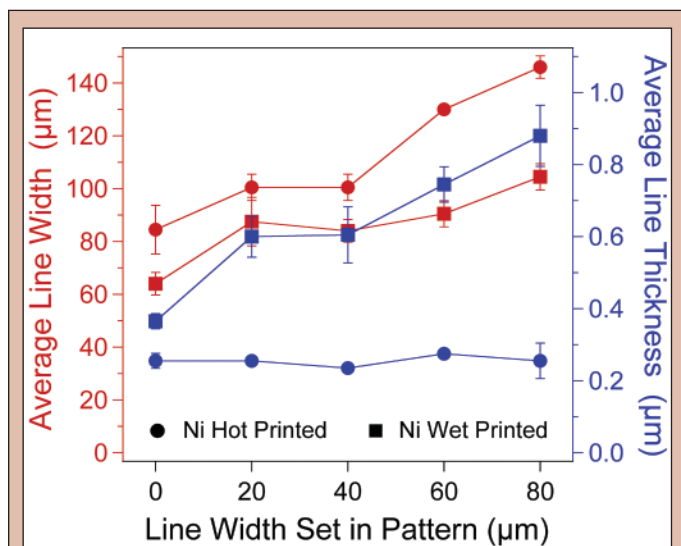


Figure 4. Line width (red) and thickness (blue) of Hot and Wet printed Ni ink at optimized 30-μm drop spacing. Single-drop-row lines printed on glass (4 layers).

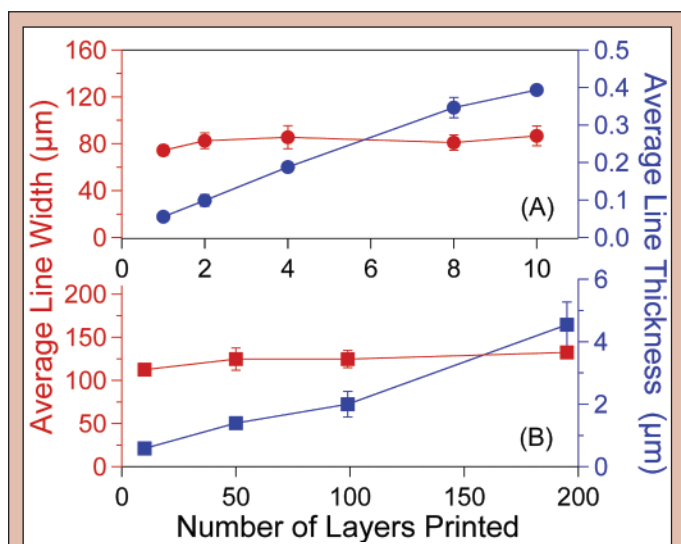


Figure 5. Line width (red) and thickness (blue) of single-drop-row lines of optimized Ni Hot Print on glass (A) and Ag on AR coated Si ribbon (B) as a function of the number of layers.

5B as a function of the number of layers printed. Figure 7 shows high-resolution Ag lines printed on glass, on inkjet printed Ni lines, on Ni foil, and on AR coated Si ribbon. The Ag ink was initially printed on glass to find the optimum drop spacing. Single rows of individual 50- μm wide Ag drops on glass at 45- μm drop spacing, just prior to line formation, is shown in Figure 7A. In Figure 7B, the fine line demonstrates that Ag can be printed on top of printed Ni lines. The wider lines are printed offset to show the Ag and Ni lines stacked.

The X-ray diffraction (XRD) patterns of the spray-printed inks for Ni, Ag, and Cu are depicted in Figure 8. The resulting metal coatings are consistent with the expected intensities and scattering angles (given by two-theta) for the pure, bulk material (included in the figure for comparison). Resistivities for the optimized Ni and Ag printed as a function of the number of layers are represented in Figure 9. The target resistivities of the pure, bulk material for Ni and Ag are $7.12 \times 10^{-6} \Omega \cdot \text{cm}$ and $1.59 \times 10^{-6} \Omega \cdot \text{cm}$ respectively [6]. Measurements were based on Ni and Ag printed using the contact pad pattern on glass and AR coated Si substrates respectively. The Si was assumed not to interfere with the resistivity measurements because the silicon nitride AR coating is a good electrical insulator.

DISCUSSION AND CONCLUSIONS

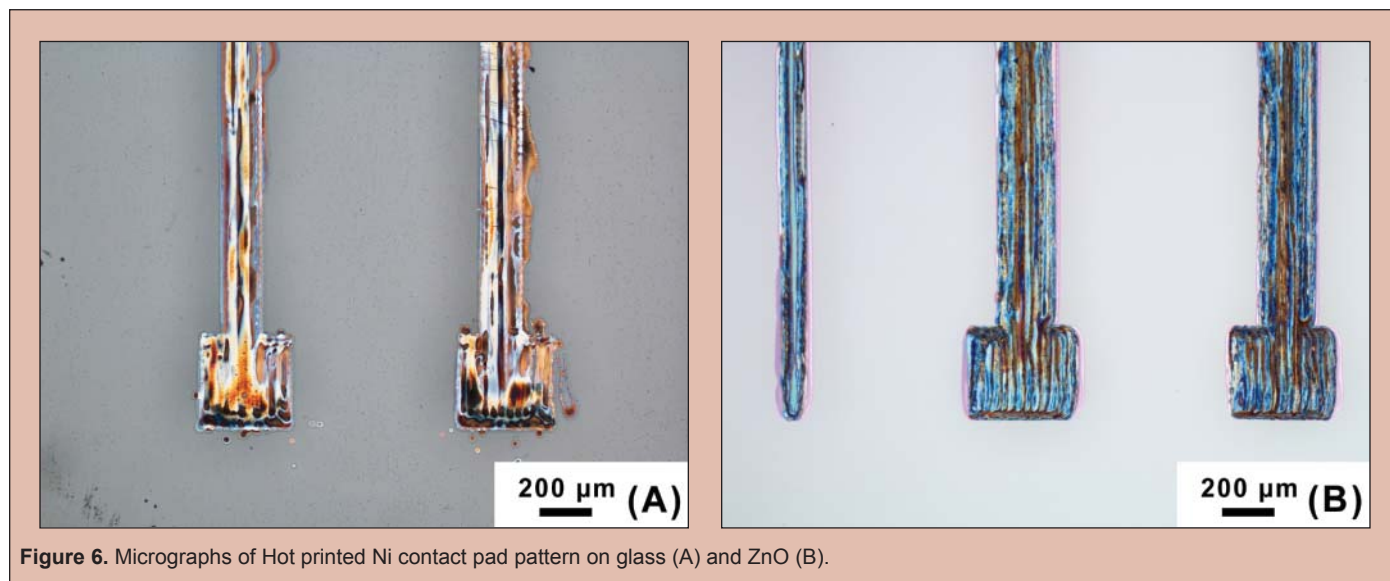
Inkjet temperature trials for the Ni ink revealed two potential avenues, referred to as the Wet and Hot Print approaches. At 140°C, the lines printed clear and were still wet. They only decomposed into black lines after secondary heating. From 150 to 170°C, the lines printed black but were still wet, suggesting that decomposition occurred without solvent evaporation. Poor quality lines that tended to bead and bubble were produced when the solvent was evaporated via secondary heating. Thus, this range was not pursued. At 180°C, dry, decomposed lines formed on contact with the heated substrate. No secondary heating was required. Above this temperature, lines tended to bubble due to the rapid evaporation of the solvent. The temperatures used for the Ni Wet and Hot Print experiments were

selected with these results in mind. Generally, the Hot Print was the preferred route since it is a simpler, single-step process. Likewise, difficulty in controlling the rate of the secondary heating for the Wet Print resulted in bubbling and line breaks.

Drop spacing was a critical parameter in the printing process because it affected line formation. At larger drop spacings (exceeding 40- μm for Ni), individual drops formed. As the drop spacing was decreased, more drops and thus material was used to create a line, which affected line thickness and width. It was crucial to find the spacing that used the least material and at which drops still merged to form a uniform line. From the experiments, the optimal drop spacing was determined to be 30 μm , at which a key difference between the two printing approaches was revealed. The thickness of the Hot Print remained unaffected by the number of rows printed next to each other while the Wet Print thickness increased (Figure 4). Ideally, one controls width only by printing more rows and controls thickness only by printing more layers.

The Ni Hot Print at 30- μm drop spacing was the superior approach because it was one-step, consistently produced continuous lines, and had more degrees of control. Hot Print Ni line width was only dependent on the number of rows printed and independent of the number of layers printed (Figure 5A). Line thickness was only dependent on the number of layers and behaved linearly, each layer adding ~50 nm of material (Figure 5A). Likewise, it met the desired features for Ni, with a width of 80 μm and thickness of 55 nm at 1 layer. The profile was consistent within each line and reproducible between lines. Figure 6 demonstrates the line quality and resolution control of features achieved on glass and ZnO. Printing parameters on ZnO were the same as on glass. Results on ZnO are promising for printing on the TCO layer in a CIS cell.

Wetting, the amount a drop spreads out on a substrate, was a critical parameter for printing Ag. Various wetting situations are illustrated in Figure 10. Initial experiments varying the drop spacing on glass revealed that individual drops formed at 45- μm (Figure 7A) and pairs of drops merged at 40- μm into larger drops. The fact that drops of ink only beaded into larger drops instead of



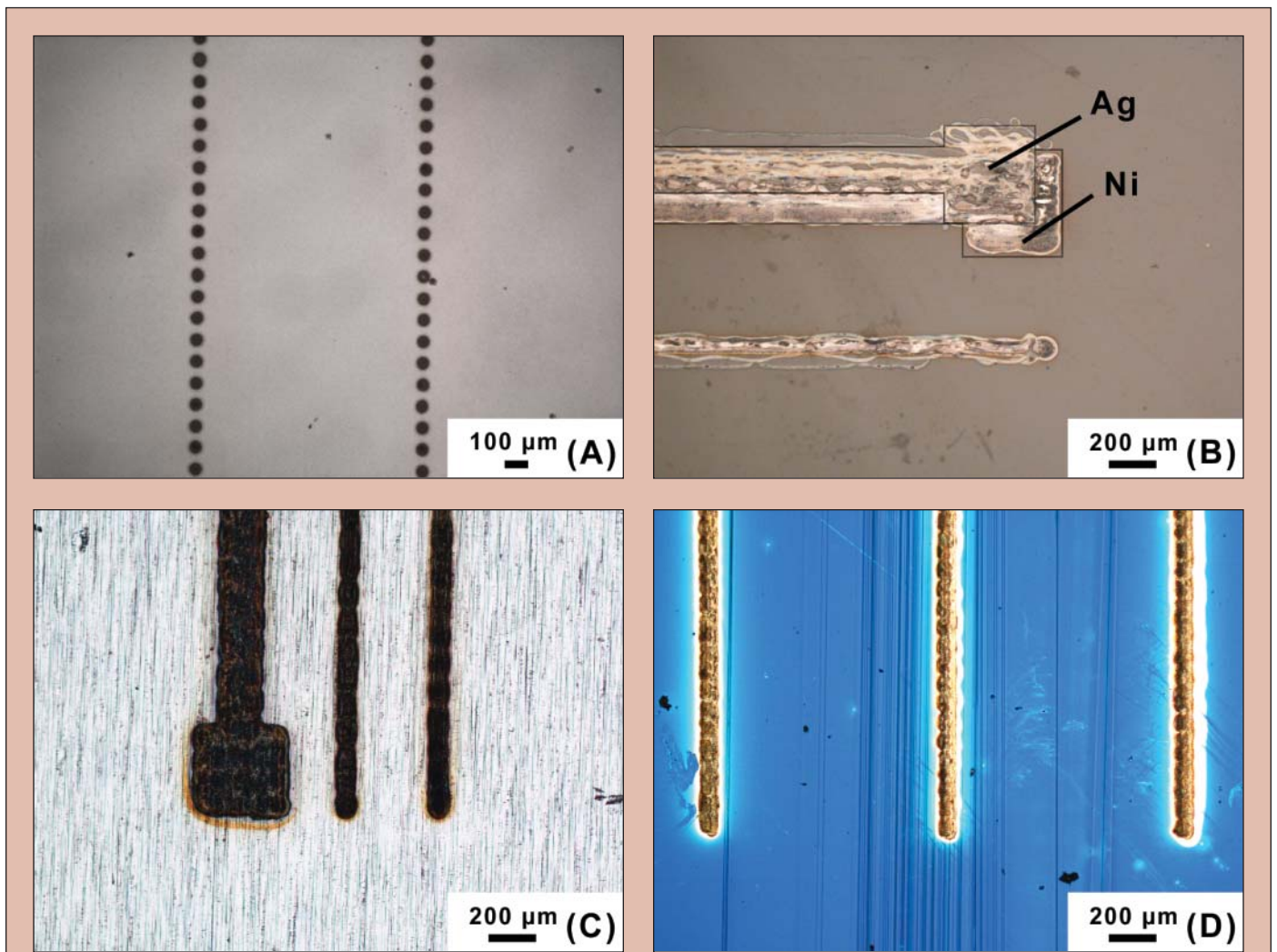


Figure 7. Micrographs of individual 50- μm wide Ag drops on glass at 45- μm drop spacing (A), Ag lines printed on top of printed Ni lines (B) and Ni foil (C), and Ag lines on AR coated Si ribbon (D).

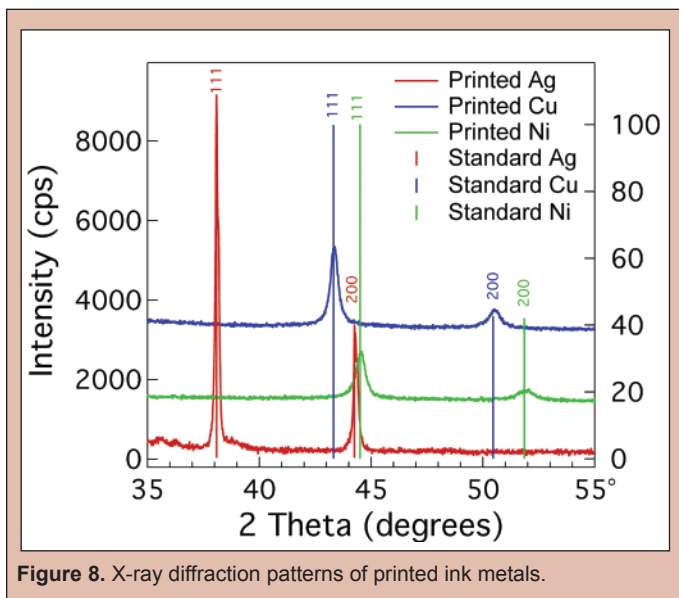


Figure 8. X-ray diffraction patterns of printed ink metals.

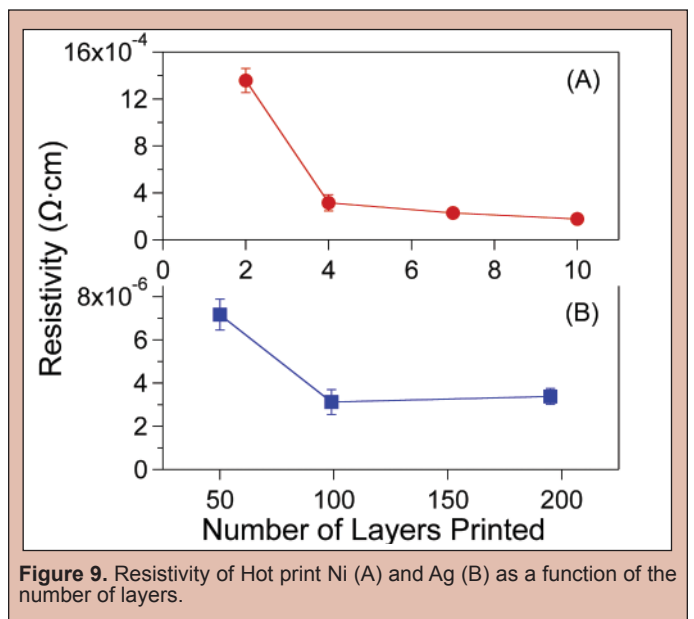


Figure 9. Resistivity of Hot print Ni (A) and Ag (B) as a function of the number of layers.

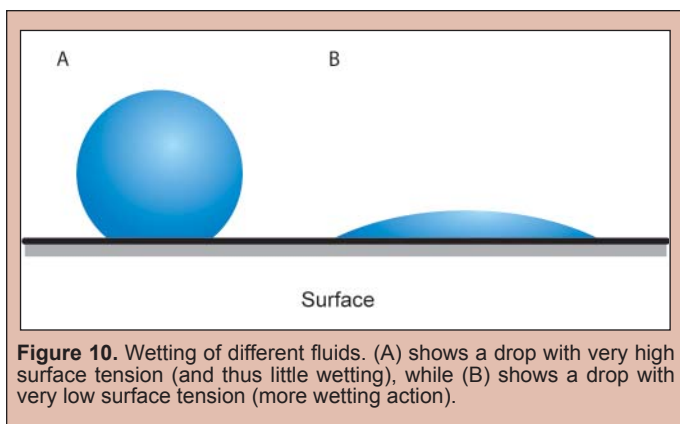


Figure 10. Wetting of different fluids. (A) shows a drop with very high surface tension (and thus little wetting), while (B) shows a drop with very low surface tension (more wetting action).

spreading to form a line indicated there was a problem with the Ag ink wetting on glass. Thus, Ni and Si were explored as substrates to observe wetting effects on materials specific for solar cell devices. Increasing the initial ink temperature by just 10°C to 45°C decreased ink viscosity, resulting in better wetting and line formation on these materials (at 35- μm drop spacing). Figure 7B shows that Ag can be printed on top of printed Ni lines. On Ni foil (Figure 7C), a smaller drop spacing (23- μm) was required to produce a single-layer line, although 30- μm printed well after 4 layers. Figure 7D shows lines form well on the AR coated Si ribbon. Results are promising for printing on the Ni layer in a CIS cell and on Si solar cells.

Ag on AR coated Si printed at a line width of $\sim 125\ \mu\text{m}$ and was unaffected by the number of layers printed (Figure 5B). Line thickness reached half its target at ~ 200 layers (4.5 μm). It should be noted that the Ag ink used was a week old and gray in the cartridge, suggesting some of the ink decomposed and that the ink printed had a lower-than-prepared precursor concentration. While the older ink still printed well, fresh ink would require fewer layers to achieve the thicknesses reported.

Metallic lines printed from the inks were consistent with the pure material and had no detectable traces of carbon or oxide contaminants, as confirmed by XRD (Figure 8). It was noted that, in addition to the purity of the metal deposited, resistivity was affected by the profile of the line. Narrow and thin features in the line limit the flow of electrons through them like a bottleneck. Therefore, uniformity in the line was an important criterion in printing contacts. Resistivity of the Ni lines decreased as more layers were printing, leveling off at $\sim 1.7 \times 10^{-4}\ \Omega \cdot \text{cm}$ at 10 layers (Figure 9A). While the value is two orders of magnitude greater than bulk Ni, the resistivity requirement of the Ni layer is relaxed since it only serves as an adhesion layer. Electrons only need to flow through the thin region of material to reach the primary Ag contact. Low resistivity is more important for the Ag since electrons must flow through the length of the contact line, similar to a wire. Ag was printed with about twice bulk resistivity at $\sim 3.4 \times 10^{-6}\ \Omega \cdot \text{cm}$ above 100 layers (Figure 9B). The Ag lines appeared white and not metallic. However, it was highly conductive like its metallic counterpart. Under certain conditions and treatment (proprietary), the white line transforms into a metallic appearance. The identity of the white material and the cause of the transformation require further study.

In summary, we have developed atmospheric direct-write depositions of Ni and Ag metals. Inkjet printing produced line

resolutions and thicknesses comparable to current screen printing technologies. Narrow (80 μm) and thin (55 nm) Ni lines were printed with a resistivity two orders magnitude more than bulk. Ag was successfully printed up to 4.5 μm thick and 125 μm wide with about twice bulk resistivity. We have shown how ink based deposition can improve the contact processing via a non-contact approach. Additionally, the ability to print on various substrates for photovoltaic applications was demonstrated on glass, AR coated Si, TCOs, and multi-layered metallizations. Future work will focus on improving Ag resolution and Ni conductivity and on printing full contact devices (TCO-Ni-Ag/Cu and Si-BurnThrough-Ag). Printing Cu will be investigated as a low-cost replacement for Ag contacts.

ACKNOWLEDGEMENTS

This research was conducted at the National Renewable Energy Laboratory. I would like to thank the Department of Energy and the Office of Science for the opportunity to participate in the SULI program and the fulfilling learning experience it provided. I extend special thanks to my mentors, Maikel van Hest and Calvin “Buzz” Curtis, for their direction, knowledge, and patience with me throughout the project. I would also like to thank Alex Miedaner for his insight and assistance in the laboratory, Xerxes Steirer for his assistance with inkjet printing, and Matthew Dabney for help with the hot plate fabrication. Additional appreciation goes to David Ginley, Ryan O’Hayre, and the entire group for their help in furthering my educational path.

REFERENCES

- [1] A. Slaoui, R.T. Collins, “Advanced Inorganic Materials for Photovoltaics,” *MRS Bulletin*, vol. 32, no. 3, p. 211, 2007.
- [2] K.F. Teng, R.W. Vest, *IEEE Electron Device Lett.*, vol. 9, p. 591, 1988.
- [3] M. Ghannam, S. Sivoththaman, J. Poortmans, J. Szlufcik, J. Nijs, R. Mertens, R. Van Overstraeten, *Solar Energy*, vol. 59, no. 1-3, pp.101–110, 1997.
- [4] T. Kaydanova, M. van Hest, A. Miedaner, C.J. Curtis, J.L. Alleman, M.S. Dabney, E. Garnett, S. Shaheen, L. Smith, R. Collins, J.I. Hanoka, A.M. Gabor, D.S. Ginley, “Direct Write Contacts for Solar Cells,” Paper presented at 31st IEEE Photovoltaics Specialists Conference, Lake Buena Vista, Florida, 2005.
- [5] A.M. Abdul-Lettif, “Investigation of Interdiffusion in Copper–Nickel Bilayer Thin Films,” *Physica B*, vol. 388, pp. 107–111, 2007.
- [6] *Handbook of Chemistry and Physics*, 65th edition, CRC Press.